The 7th International Supercritical CO_2 Power Cycles Symposium
February 21 – 24, 2022, San Antonio, Texas
Paper 188

Thermodynamic assessment and optimisation of supercritical and transcritical power cycles operating on CO_2 mixtures by means of Artificial Neural Networks

Pablo Rodríguez de Arriba
PhD Student
University of Seville
Seville, Spain

Francesco Crespi*
Lecturer
University of Seville
Seville, Spain

David Sánchez
Full Professor
University of Seville
Seville, Spain

Pablo Rodríguez de Arriba is a Ph.D. Student in Energy Engineering at the University of Seville. He obtained a Master's Degree in Industrial Engineering in 2020 and joined Prof. David Sánchez's Research Group as Research Assistant since then. His thesis is focused on the techno-economic optimisation and integration of innovative CO_2-based technology for Concentrated Solar Power applications, within the framework of the SCARABEUS project. His areas of interest also include thermodynamics, heat transfer, non-conventional working fluids, renewable energies, desalination, WHR and refrigeration.

Francesco Crespi is a lecturer in Fluid Mechanics at the University of Seville, where he currently works at the Department of Energy as a postdoctoral research associate. Dr. Crespi started his research activity at the beginning of 2015 after completing a Double Degree in Industrial Engineering from University of Seville and Politecnico of Milan. His research activity at the moment is focused on numerical simulation of sCO_2 power cycles, alternative cycle layouts for this technology and analysis of possible dopant candidates for CO_2 blends.

David Sánchez is a Full Professor in Energy Systems and Fluid Machinery at the University of Seville, where he currently works at the Department of Energy Engineering. He has fifteen years' experience in the field of stationary power generation using turbomachinery in combination with novel cycle concepts that can introduce step-changes in the Concentrated Solar Power industry, thus enabling higher efficiencies and lower electricity costs. He has conducted research to integrate the sCO_2 power cycle into CSP and WHR applications for more than ten years, with both private and public funding at the fundamental and applied levels.

ABSTRACT

Closed supercritical and transcritical power cycles operating on Carbon Dioxide have proven to be a promising technology for power generation and, as such, they are being researched by numerous international projects today. Despite the advantageous features of these cycles enabling very high efficiencies in intermediate temperature applications, the major shortcoming

of the technology is a strong dependence on ambient temperature; in order to perform compression near the CO_2 critical point (31ºC), low ambient temperatures are needed. This is particularly challenging in Concentrated Solar Power applications, typically found in hot, semi-arid locations.
To overcome this limitation, the SCARABEUS project explores the idea of blending raw carbon dioxide with small amounts of certain dopants in order to shift the critical temperature of the resulting working fluid to higher values, hence enabling gaseous compression near the critical point or even liquid compression regardless of a high ambient temperature. Different dopants have been studied within the project so far (i.e. C_6F_6, $TiCl_4$ and SO_2) but the final selection will have to account for trade-offs between thermodynamic performance, economic metrics and system reliability.
Bearing all this in mind, the present paper deals with the development of a non-physics-based model using Artificial Neural Networks (ANN), developed using Matlab's *Deep Learning* Toolbox, to enable SCARABEUS system optimisation without running the detailed – and extremely time consuming – thermal models, developed with *Thermoflex* and *Matlab* software.
In the first part of the paper, the candidate dopants and cycle layouts are presented and discussed, and a thorough description of the ANN training methodology is provided, along with all the main assumptions and hypothesis made.
In the second part of the manuscript, results confirms that the ANN is a reliable tool capable of successfully reproducing the detailed Thermoflex model, estimating the cycle thermal efficiency with a *Root Mean Square Error* lower than 0.2 percentage points. Furthermore, the great advantage of using the Artificial Neural Network proposed is demonstrated by the huge reduction in the computational time needed, up to 99% lower than the one consumed by the detailed model. Finally, the high flexibility and versatility of the ANN is shown, applying this tool in different scenarios and estimating different cycle thermal efficiency for a great variety of boundary conditions.

INTRODUCTION

sCO_2 technology has gained increasing interest among in the scientific community in the last twenty years, and is now the focus of several international research projects for very different applications, such as Concentrated Solar Power (SCARABEUS [1], COMPASSCO2 [2]), fossil fuels (sCO_2 flex [3]), heat removal from nuclear plants (sCO_2-HeRo [4], sCO_2-4-NPP [5]) and Waste Heat Recovery (I-ThERM [6] , CO2OLHEAT [7]). Among the virtues of sCO_2 power cycles stand out their high thermal efficiency, low footprint in comparison to conventional steam and gas turbines cycles and operational flexibility [8]. The major drawback of this technology is that low ambient temperatures are needed in order to perform compression near the critical point (31ºC), thus taking advantage of a low compressibility factor. Nevertheless, this is particularly difficult to obtain considering in Concentrated Solar Power (CSP) applications, which are typically situated in hot, semi-arid locations.

An alternative solution to overcome this limitation is proposed by SCARABEUS project, whose main concept is to investigate the possibility of blending raw carbon dioxide with certain dopants in order to increase the critical temperature of the resulting working fluid, enabling its condensation at high ambient temperature and thus enhancing cycle thermal performance. Three different dopants have been studied in the framework of SCARABEUS project so far – Hexafluorobenzene (C_6F_6), Titanium tetrachloride ($TiCl_4$) and Sulphur Dioxide (SO_2) – and the main outcomes regarding the identification of the best performing cycle layout when each one of these dopants is employed has been already disclosed in the public domain [9], [10]. Nevertheless, the final selection will have to account for trade-offs between thermodynamic performance, economic metrics and system reliability: in other words, a thorough overall system optimization.

System Optimization of power plants is a wide task with multiple scopes, ranging from power block *thermodynamic Optimization,* usually aimed to maximize thermal efficiency, to techno-economic optimization, with the objective of minimizing the Levelised Cost of Electricity (LCoE) of the entire plant. Moreover, other figures of merits such as environmental or social indicators can be taken into account besides economic metrics in order to perform a multi-objective optimization of the technology (*Techno-economic-environmental Optimization*).

Simulation of power cycles operated near the critical point is highly time-consuming. Convergence is low due to the extreme non-linearity of fluid properties and heat balances [11]. For example, heat exchangers have to be divided in sub-sections in order to account for the high variation of heat capacity [12]. Computational time of such systems are in the order of 10^1 seconds [13]. An optimization routine to find the set of operational variables maximizing thermal efficiency requires around 100 iterations, therefore, 10^3 seconds for a single operating point optimization. Annual calculations require 8760 simulations of more complex models that account for off-design performance and operational strategies. This number can be reduced to a few hundred by mapping the cycle off-design performance as a function of the ambient temperature, HTF temperature and HTF mass flow rate, for example, as requested by System Advisor Model. Even if the computational time remains in the order of 10^1 seconds (although it is very likely to grow due to the increase in the number of nested iteration loops), a single yearly simulation would last 10^3-10^4 seconds. What is more, different configurations –in the order of thousands [14]- have to be studied in order to minimize the LCoE. If multiple objective functions were to be considered, generating the Pareto Front would require the use of Metaheuristic Algorithms (e.g., genetic algorithms) and between 5000 and 10000 yearly simulations. In summary, directly optimizing the detailed model leads to prohibitive simulation times.

Bearing all this in mind, the present manuscript deals with the creation and development of a surrogate model based on Artificial Neural Networks, which enables to reduce the optimization time by various orders of magnitude [14]–[16]. In this context, it is worth noting the novelty of the proposed approach, which results to be different from other similar investigations published in literature. In [17], [18] the authors studied the *Recompression Cycle* with sCO_2 for nuclear applications. In these studies, a *Parametric Optimization* is performed, meaning that the system has been first directly optimized by means of a Genetic Algorithm for different conditions and the results of such optimization constitutes the training set provided to the Neural Network. In the present work, the ANN will completely replace the detailed model and the optimization will be performed *ove*r the ANN and not *on* the detailed model. A similar investigation is presented in of [19], where a Neural Network is trained with data obtained with a detailed model for different boundary conditions. Nevertheless, the system thereby studied was a *Recuperated Rankine Cycle* for low-grade Waste Heat Recovery (TIT < 100ºC) running on different working fluids. Thus, to the authors knowledge, this is the first time that ANNs are used as surrogate models for the optimization of CO_2-based power cycles for Concentrated Solar Power applications.

The structure of the manuscript is the following: the first part introduces three dopants studied within the SCARABEUS project, namely C_6F_6, $TiCl_4$ and SO_2, along with a brief discussion on the best-performing cycle layout for each working fluid. The second part deals with the development of a comprehensive methodology for the optimization of complex, time-consuming energy models using ANN and applies it to the analysis of sCO_2-based power cycles. The computational time invested in generating the training set and training the surrogate model is compensated with extreme flexibility. Finally, the results obtained with the ANN are compared with the ones achieved by the detailed model, developed with the commercial software *Thermoflex*, showing the reliability of the proposed ANN, which is proven to be capable of reproducing the results of the detailed model with a great accuracy but with an extremely lower computational time needed.

CANDIDATE DOPANTS

As previously commented in the introduction, three different candidate dopants are considered in this work - C_6F_6, $TiCl_4$ and SO_2 – and their main thermophysical properties are provided in Table 1. It can be easily noticed that the critical temperatures of these compounds are considerably higher than the one of pure CO_2 (186ºC for C_6F_6, 190ºC for $TiCl_4$ and 64ºC for SO_2), being this the key feature that enables condensation of the resulting mixtures at temperatures equal or higher than 50ºC. A discussion regarding the safety issues related to these dopants, based on the NFPA 704 standards, can be found in previous papers by the same authors [9]. A special comment must be made on dopant thermal stability, currently being investigated by other partners of SCARABEUS consortium (University of Brescia and Politecnico di Milano). The complete set of results of this research activity will be disclosed in the near future by these institutions and cannot be hereby discussed due to confidentiality issue, but the main conclusions are presented in Table 1. On one hand, very promising results have been obtained for $TiCL_4$, for which thermal degradation is observed only for temperatures above 700ºC. Almost no preliminary results have been obtained for CO_2 and SO_2, which are currently being tested, but different references from literature depict a very promising scenario, with foreseen thermal stability for temperatures higher than 700ºC [20]. On the other hand, the same cannot be said for C_6F_6, which shows some signs of thermal degradation for temperatures above 600/625ºC. Nevertheless, it is worth noting that this is merely a preliminary results and this threshold value needs further investigation to be confirmed. For this reason, in the present paper TIT values higher than 625ºC are taken into account, in order not to limit the analysis and compare the ANN reliability when employed to foresee the thermal performance obtained with the three dopants with the same set of boundary conditions. Nonetheless, if C_6F_6 thermal stability will be confirmed to be limited to 625ºC, this would be the maximum TIT level to be considered for techno-economic optimization, and this would undoubtedly be an important drawback for this dopant.

Table 1. Thermo-physical properties of pure CO_2, C_6F_6, $TiCl_4$ and SO_2

	CO_2	**C_6F_6**	**$TiCl_4$**	**SO_2**
MW [kg/kmol]	44.01	186.06	189.69	64.06
Tcr [ºC]	31.06	243.58	364.85	157.60
Pcr [bar]	73.83	32.73	46.61	78.84
Thermal stability	Up to 700ºC	Up to 625ºC	>700ºC	>700ºC
BIP	-	0.16297 - 0.0003951·T	0.0704	0.0242

Thermo-physical properties of the mixtures have been obtained with Aspen v11 [21], employing Peng-Robinson's Equation of State with Van der Walls mixing rule. The binary interaction parameters (BIP, see last row in Table 1). have been calibrated on experimental data available in Aspen library. Further information regarding properties estimation can be found in previous papers by SCARABEUS Consortium [9], [22], [23] . The critical loci of the three mixtures are presented in Figure 1, highlighting the range of molar fraction of dopant employed in the present study: 10%-20% for C_6F_6, 15%-25% for $TiCl_4$ and 20-40% for SO_2. These candidate ranges of dopant molar fraction were identified in previous works by the authors, and are based on a twofold criterion: i) maximize cycle thermal efficiency, ii) guarantee a gap in the order of 30ºC between minimum cycle temperature and mixture critical temperature, in order not to operate compression in the extreme vicinity of the critical point.

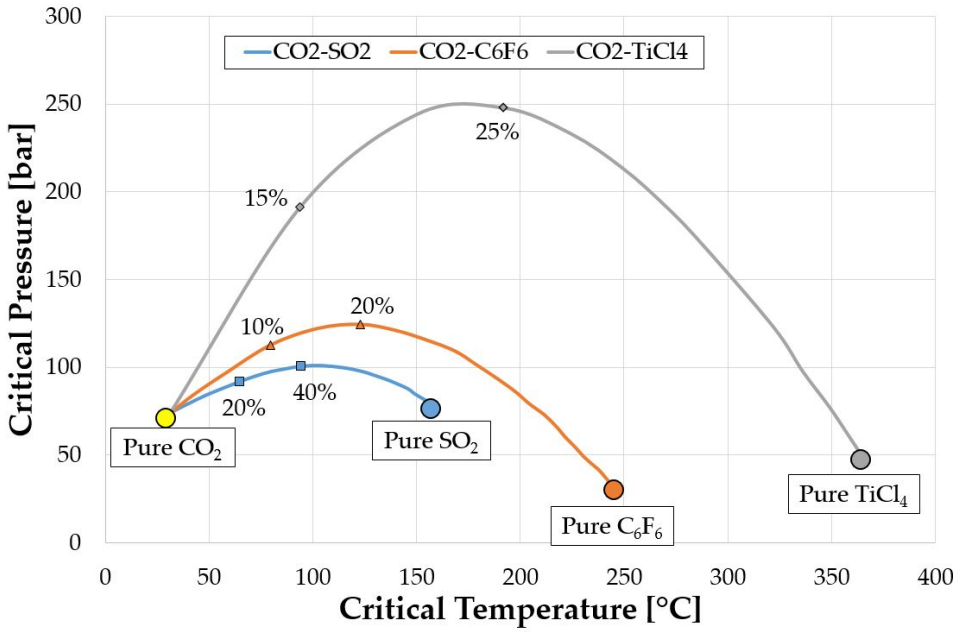

Figure 1. Critical Loci of SCARABEUS mixtures. Candidate ranges of dopant molar fraction are indicated by markers.

CANDIDATE CYCLE LAYOUTS

Three different candidate cycles are considered for SCARABEUS mixtures, previously identified in a work by the authors by means of a thorough screening of sCO_2 cycle layout proposed in literature [10]: the simple recuperated (hereby called *Recuperated Rankine*), the *Precompression* and the *Recompression* cycle, whose layouts are presented in Figure 2. For the three dopants considered, the optimum combinations of cycle layout and working fluid, as identified in previous works for a minimum cycle temperature of 50ºC (SCARABEUS reference case), are: *Precompression* with 15% molar fraction of C_6F_6, *Recuperated Rankine* with 15% of $TiCl_4$ and *Recompression* with 30% of SO_2.

Interestingly, these three configurations were originally proposed by Gianfranco Angelino in its seminal work [24]–[26], in a very similar transcritical embodiment as the one considered in the present work. The transcritical nature of SCARABEUS cycles, to which from now on we will add the adjective "*transcritical*" to differentiate them from the typical supercritical embodiment of pure CO_2 cycles, is due to the fact that the addition of certain dopants enables the condensation of the working fluid for temperature levels higher than 31ºC (critical temperature of CO_2). This fact, besides the obvious need for a main pump and a condenser instead of a main compressor and cooler, leads to an extremely interesting side-effect: in transcritical cycles, the main pump inlet pressure is no longer a free/optimizable parameter, but it is constrained by the minimum cycle temperature through the bubble point (condensation process). Actually, the condensing pressure can indeed be changed by means of an innovative degree of freedom - the molar fraction of dopant – but at the expense of considering different thermodynamic behavior of the mixture and, from a practical point of view, changing the working fluid. On the contrary, for supercritical cycles, that pressure level is a further degree of freedom for optimization, which allows to change the heat capacity of the low pressure stream – in order to balance the heat capacities in the heat regeneration - at the expense of penalizing specific work.

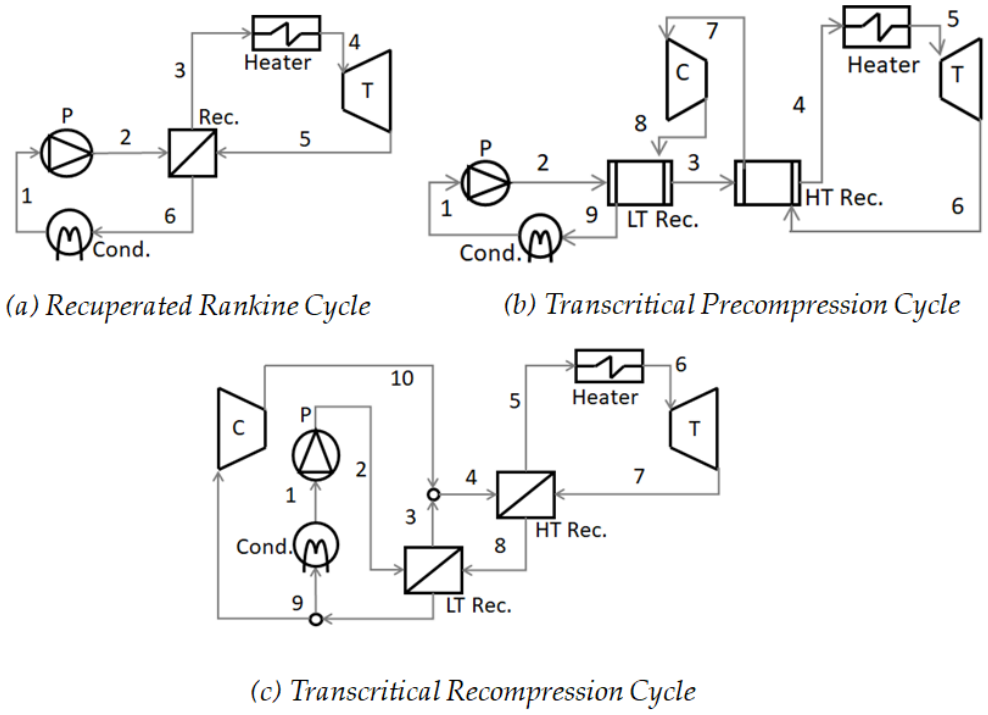

Figure 2. Candidate cycles for SCARABEUS concept

Bearing this in mind, the same cycle layout can behave in a very dissimilar way depending if it is considered in a transcritical or supercritical embodiment. In order to fully appreciate these different behaviors, a series of crucial cycle parameters which plays a fundamental role in its thermodynamic optimization are hereby identified and discussed, and their effects are resumed in Table 2. It is worth remarking the fact that these parameters will be part of the complete set of input variables considered in the ANN (see next sections of the paper).

The *Main Compressor Inlet Pressure* allows to change the proximity to the critical point in supercritical power cycles. This allows to balance the benefits (low compressibility factor, higher Pressure Ratio) and disadvantages (irreversibilities in the heat regeneration) of working near the critical point. In transcritical cycles, this pressure level is fixed by the cycle temperature through the bubble point. The *molar composition* has a similar but conceptually different impact: instead of varying main pump inlet conditions, it allows to shift the critical point itself. Additionally, different composition of the same dopant has different condensing pressure for the same bubble temperature, thus having an effect on the Pressure Ratio. The *split-compression* works similarly in both transcritical and supercritical cycles: at the expense of a lower specific work, the heat regeneration is improved by reducing the heat capacity of the high pressure stream. The addition of a *Pre-compressor* in transcritical configurations permits to overcome the limitation imposed by pump inlet pressure on turbine exhaust, hence increasing cycle specific work. On the contrary, in supercritical configurations, this cycle modification causes a rise in main compressor inlet pressure, resulting in an enhanced heat recuperation process (balancing heat capacities, reducing internal irreversibilities). This leads to a rise in cycle thermal efficiency, but with an overall detrimental effect in terms of specific work. In fact, the direct consequence is that main compressor inlet is shifted away from the critical point, resulting in a significant rise in compression power. Finally, the effect of *Maximum Cycle Pressure* is very similar for both transcritical and supercritical embodiments, and can be optimized in order to maximize either thermal efficiency or specific work.

Table 2. Comparison between the degrees of freedom of transcritical and supercritical power cycles

	Transcritical	Supercritical
Main Compressor (Pump) Inlet pressure	Set by Minimum Cycle Temperature through the bubble point (condensation process).	Further degree of freedom: compromise between cycle specific work and recuperator performance
Molar Composition	Shift in critical point of mixture: affects to both thermo-dynamic props and pump inlet pressure	Only pure fluids are considered for supercritical cycles.
Split compression factor	Improves internal heat recovery and harms specific work.	Improves internal heat recovery and harms specific work.
Precompressor pressure ratio	Overcomes the limitation on turbine exhaust pressure, increasing both thermal efficiency and specific work.	Beneficial effect on thermal efficiency, detrimental for specific work
Maximum Cycle Pressure	Affects specific work and available energy for regeneration at turbine exhaust	Affects specific work and available energy for regeneration at turbine exhaust

COMPUTATIONAL ENVIRONMENT

In order to allow an easier combination with the ANN, cycle simulations have been completed with various in-house codes written in Matlab R2021a [27], thoroughly validated with the results obtained with Thermoflex [28] and already presented in previous works by the same authors [9], [10]. As afore-commented, the layouts considered for transcritical power cycles (i.e., SCARABEUS working fluids) are the *Recuperated Rankine Cycle, Transcritical Precompression Cycle* and the *Transcritical Recompression Cycle*. Moreover, two well-known pure sCO_2 cycles have also been studied for sake of comparison: *Recompression Cycle* and *Partial Cooling Cycle*, considered as representative for pure sCO_2 technology. The same set of boundary conditions has been employed for both pure and blended configurations, and it is hereby provided in Table 3. On the other hand, different values of Turbine Inlet Temperature, Minimum Cycle Temperature and Maximum Cycle Pressure are taken into account, as specified in Table 4.

Table 3. Complete set of fixed boundary conditions

Gross Output [MW]	$\eta_{is,T}$ [%]	$\eta_{is,C}$ [%]	$\eta_{is,P}$ [%]
100	93	89	88

ΔT_{min} [ºC]	ΔP_{PHX} [%]	ΔP_{HRU} [%]	ΔP_{REC} [%] low/high P side
5	1.5	1.0	1.0/1.5

Thermodynamic properties of the candidate blends, previously obtained with Aspen software, have been introduced in Matlab codes by means of look-up tables for fixed molar compositions:

for C_6F_6, dopant molar fractions from 10-20% with a step of 1%; for $TiCl_4$, from 15-25% with 1% step; and for SO_2 from 20-40% with 2% step.

ARTIFICIAL NEURAL NETWORK

Artificial Neural Networks have been modelled using Matlab's Deep Learning Toolbox [29]. The training set have been generated using the Matlab codes. The ranges of the various parameters sampled for the generation of the training sets are shown in Table 4. Minimum Cycle Temperature accounts for different locations (ambient temperature) from mild (35ºC, lower bound) to hot (60ºC, upper bound) climates. Turbine Inlet Temperature refers to both state-of-the-art of CSP plant (550ºC, lower bound) as well as advanced CSP receiver temperatures (700ºC, upper bound). Maximum Cycle Pressure stands as a technological boundary condition for current materials (250 bar, lower bound) and advanced material constraints (350 bar, upper bound). The remaining ANN training set limitations (e.g. Precompressor pressure ratio, split flow factor[1] etc.) have been fixed considering the results obtained in previous research activities by the authors [9].

Table 4. Ranges of the various parameters sampled during the generation of the ANN training sets

	Lower bound	**Upper bound**	**System**
Minimum Cycle Temperature [ºC]	35	60	All
Turbine Inlet Temperature [ºC]	550	800	All
Maximum Cycle Pressure [bar]	250	350	All
Molar fraction C_6F_6 [%]	10	20	*Transcritical Precompression with CO_2-C_6F_6*
Molar fraction $TiCl_4$ [%]	15	25	*Recuperated Rankine with CO_2-$TiCl_4$*
Molar fraction SO_2 [%]	20	40	*Transcritical Recompression with CO_2-SO_2*
Precompressor PR [-]	1.0	1.6	*Transcritical Precompression with CO_2-C_6F_6*
Split-flow factor [-]	0	0.6	*Transcritical Recompression with CO_2-SO_2*
Main Compressor PR [-]	1.5	4	*sCO_2 Recompression / Partial Cooling*
Precompressor PR [-]	1.0	2.5	*sCO_2 Partial Cooling*
Split-flow factor [-]	0	0.6	*sCO_2 Recompression*

[1] Note that split-flow factor of a *Recompression* cycle (either transcritical or supercritical) refers to the fraction of working fluid that flows through the re-compressor. Thus, if this value is set to zero, the *Recompression* cycle is practically transformed into a *Simple recuperated* cycle.

An Artificial Neural Network (also called Neural Network, ANN) is a mathematical model inspired by the working of a biological brain. A brain is built form a massive number (more than 10^{11}) of interconnected units called *neurons*. The resulting structure is both capable of storing and processing information. To that end, the brain modified the arrangement of the neurons (connections can grow) and the strength of these links (called *synapses*). ANN cannot achieve such complexity but it resembles some of its key operating principles: (1) they are formed by a large number of simple units, (2) they can learn from the environment, and (3) the knowledge can be stored inside the network by modifying the weights of the connections. Artificial Neural Networks can be used in a broad range of applications fields from engineering to finance or even literature [30]. In this work, ANN are used to replicate the behavior of a physical model. This problem is called *function approximation*, meaning that the ANN is asked to create a mapping between the inputs and the targets, identifying the hidden dynamics underlying between them [31].

The fundamental unit of an ANN is the *neuron* (Figure 3). It is a mathematical element that receives, processes and transfers information. More specifically, it collects a vector of I inputs (x) and transforms it into the scalar y. To do so, neurons count on three elements. The *synaptic connections* collect all inputs and assign a weight to each one of them; the *Adder* sums up the weighted inputs and then add a threshold value called *bias*; and, finally, a *Transfer (activation) function* that transforms the output from the adder into the output of the neuron. The transfer function is chosen depending on the problem that wants to be solved, it can either be linear/non-linear or discrete/continuous. The most important types are *Threshold Functions* (not used in function approximation but for pattern recognition), *Linear Functions* (the output is equal to the input) and *Sigmoid Functions* (S-shaped functions with two horizontal asymptotes).

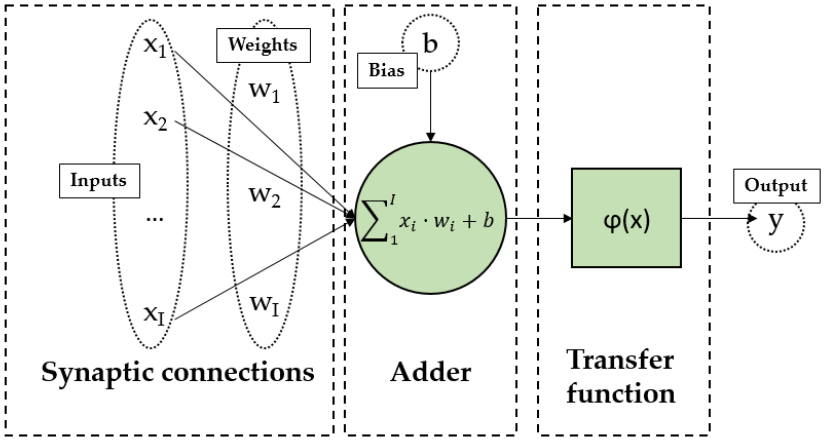

Figure 3. Neuron scheme

Neural Network consists of multiple neurons connected between them. Neurons are organized in parallel forming a layer, while layers are arranged in series giving place to the network. Three types of layers are identified: *Input layer*, which does not transform the information in any way but distributes into the network; the *Output layer*, which produces the output of the network; and the *Hidden layer(s)*, which are found between the *Input* and *Output layers* and are actually responsible of the computational power of ANN. The type of Neural Network studied for function approximation problems is the *Multilayer Feedforwards Network*. In this configuration, the information flows only in one direction, from the *input layer* to the *output layer* through the *hidden layer(s)*. Moreover, the network will be *fully-connected*, meaning that the output from all the

neurons of a layer are the inputs of the neurons of the consecutive layer. Figure 4 shows a Neural Network as described before with two hidden layers and only one output.

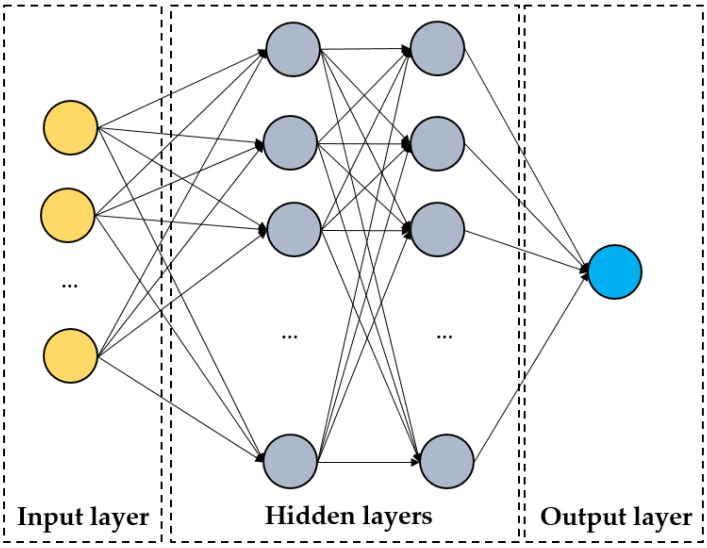

Figure 4. Multilayer Feedforward Neural Network, with two hidden layers and one output

The *Universal Approximation Theorem* [30] (pag. 230-231) states that a Multilayer Feedforward Network with at least one hidden layer with a sigmoid function as transfer function and an output layer with a linear function is a universal approximator. This means that an ANN of that characteristics is potentially able to approximate any continuous function. This theorem provides the mathematical justification that the present problem we are trying to solve does actually have a solution. However, the path for obtaining that solution is far from being trivial. The process by which a network adjusts its free parameters to improve its performance is called *Training* and, as described below, it is something much broader than using a training algorithm.

The free parameters of a neural network correspond to the weights and biases of each neuron. Considered a network of I neurons in the input layers, h hidden layers with H_i neurons in the hidden layer i and only one output. The total number of free parameters, n, is expressed in Equation 1. The first term corresponds to the number of biases (equal to the total number of neurons except from the neurons in the input layer). The second term is the number of synaptic connections: $I \cdot H_1$ are the connections from the input layer to the first hidden layer, H_h are the connections from the last hidden layer to the single neuron in the output layer and the last term are the connections between the remaining hidden layers.

$$n = \left(\sum_{1}^{h} Hi + 1 \right) + \left(I \cdot H_1 + H_h + \sum_{2}^{h-1} H_i \cdot H_{i-1} \right) \qquad (Eq. 1)$$

A standardized methodology to train ANN cannot be found among the scientific literature. In this work, a comprehensive methodology is proposed, gathering multiple parameters the designer has to consider to properly trained (i.e. maximize the performance) an ANN.

The authors have identified the followings:

- Sampling method and sampling size.

- Number of hidden layers and neurons in each layer (ANN architecture).
- Transfer function in the hidden layer.
- Normalization method of the data in the training set.
- Figure of merit employed to quantify the performance.
- Training algorithm.
- Data division.
- Number of re-trainings.

A sufficiently large set of simulations have to be provided to the network so it can learn the underlying dynamics between input and targets. Sampling of the detailed model is the high time-consuming task of the optimization using ANN, therefore only the minimum number of simulation should be performed. To that purpose, the input domain should be optimally sampled in order to maximize the information contained in the training set. In this work, the simple *Uniform Random* Sampling (or *Montecarlo* Sampling) is employed. Other methods include the *Systematic* Sampling or the *Latin-Hypercube* Sampling [32]. The main advantage of the selected method is its modularity: as each sample is chosen independently from each other, the sampling size can be progressively increased in order to find the minimum amount that yields a certain level of error. The superiority of the *Latin-Hypercube Sampling* is not clear because, although it guarantees one-dimensional projection properties, the sample does not have to be uniformly distributed through the n-dimensional space. For its part, the *Systematic Sampling* do ensure a space-filled sample, but not one-dimensional projection.

Regarding the architecture of the ANN, it can only be chosen by means of a sensitivity analysis. A *Shallow Neural Network* (i.e. one hidden layer) should always be studied first. If the error required cannot be achieved by such network, *Deep Neural Network* with two hidden layers are to be considered. More than two hidden layers are hardly ever necessary. It has to be pointed out that the training time scales exponentially with the number of hidden layers, as well as the risk of overfitting the data. In this study, constant architecture sizes are tested, acknowledging that small variations in the number of neurons have little impact on the performance of the network [33]. Some authors have also performed a sensitivity to the transfer function used in the hidden layers. However, the hyperbolic tangent sigmoid function is one of the most used in recent literature publications [16], [34]–[36].

Data can rather be provided to the network in its original units or be normalized to ease the training process. Two normalization method are discussed in literature: the [-1,1] normalization and the [0 mean, 1 variance] normalization [31]. The idea behind normalization is to move the range of the data closer to the region in which the sigmoid functions are not saturated (usually between -3 and 3), so the gradients in the first iterations of the training are significant from the very beginning. Normalization is a standardized practices and the [-1,1] normalization will be applied in this work.

Several different figures of merit exist for measuring the performance of the trained Network. Some examples are the *Mean Square Error (MSE)*, the *Root Mean Square Error (RMSE)*, the *Mean Percentage Error (MPE),* the *Mean Absolute Percentage Error (MAPE)*, the *Coefficient of Variation (CoV)* or the *Coefficient of Determination (R^2).* There is no a uniform preference in literature, for each one measures different aspect of the performance. In this study, the RMSE is selected because it is measured in the original units of the target, thus representative of the uncertainty predictions of the surrogate model. RMSE can be calculated according to Equation 2, where n is the total number of samples, t is the target shown to the network and y is the value predicted by the network.

$$RMSE = \sqrt{\frac{1}{n}\sum_{i=1}^{n}(t_i - y_i)^2} \qquad (Eq.2)$$

Once the previous information has been selected, the training process consists in finding the optimum values for the weights and biases so the error between targets and predicted outputs is minimized. Training an ANN is far from being a deterministic process. On the contrary, the free parameters of the network are initialized randomly. The two most employed training algorithm are the *Levenberg-Marquardt* and the *Bayesian Regularization*, which are both a *Backpropagation algorithm based on the Newton's Method* but with different stopping criteria [31]. The former is based on early-stopping, meaning that a set different from the training and test (called validation set) is used to stop the training process before the network starts to overfit (i.e., memorize the patterns instead of learning the relations between them) the data. In the latter, the definition of the performance function is changed to penalize the complexity of the network (i.e. the amount of free parameters employed). The advantage of the *Bayesian Regularization* is that it only uses as many free parameters as necessary, no matter if the architecture of the network is more complex. On the other hand, the *Levenberg-Marquardt algorithm* is significantly faster, therefore suitable for extensive sensitivity analysis.

The full data set has to be divided in, at least, two sets: a training set and a test set. The former is used during the training to adjust the free parameters of the net, whereas the latter is employed to assess the performance of the trained net, thus to evaluate its generalization capability (i.e. ability to produce outputs with a good resemblance to the real model for inputs that have not been shown during training). If the *Levenberg-Marquardt algorithm* is selected, the aforementioned validation set is also required. Ideally, all data sets should be statistically representative of the whole space explored. Otherwise, the training can be inefficient in the sense that the network is not shown the complete picture of the system dynamics- thus it is not able to generalize well, or, on the other hand, the test error could be over or under-estimated as a result of there being more points in the test data from a region which is easy or harder to predict. Additionally, this problem can also occur if the test set is too short. A well trained network has a test error usually higher than the train error, both decreasing during the training process. Two decisions have to be made in this stage: the percentages designated to each set and which particular simulations will conform them. If the number of samples is sufficiently high, then randomly dividing the data can be assumed to maintain the statistical representativeness of the data. An alternative is to individually select a sampling for the test set (and validation) following any of the sampling methods mentioned before. In this work, the training algorithm is the *Levenberg-Marquardt* with a 70/15/15% division between train, validation and test sets, respectively, as widely employed in literature [34], [36]–[38]. However, future works have to focus in quantifying how this critical step, along with the sampling method, affect the minimum number of samples required for achieving a certain level of accuracy.

Training of an Artificial Neural Network is nothing more but an optimization problem. Nevertheless, given that the error function is extremely non-linear, the solution achieved during training will probably be a local optimum. To avoid falling in local optima, it is recommended to repeat the training process a sufficient number of times. Some comments have to be made about re-training. First, some criteria are needed to choose among the multiple networks. The network with the lowest train set error (global optimum) cannot be selected because it will probably overfit the data (have a large error in the test set). Consequently, in this work, the trained net with the lesser test error is selected, always provided that it is larger than the total error. Secondly, as it cannot be guaranteed that the test set is statistically representative of the design space, there is a risk, if the number of re-trainings is too large, of accidentally selecting a solution that overfits

both the train and test sets, this problem is called *overfitting due to model selection* [39]. After some sensitivity studies, a number of 25 re-trainings have been chosen as a trade-off between finding a good local optimum and avoiding overfitting. Nevertheless, this is not a golden rule and do not exempt the designer of manually assessing the obtained network.

Finally, it is worth remarking that the optimum values for the weights and biases do not depend on the training algorithm chosen, neither the number of re-training, nor the training set, nor the normalization method. These parameters affect how closely (and consistently) the solution found during training resembles the global optimum, but the potential performance of the ANN as a surrogate model only depends on the number of hidden layers and neurons and the activation function selected (which defines the mathematical description of the ANN).

All design criteria has been summarized in Table 5.

Table 5. Decision parameters and its corresponding value

Decision parameter	Value
Sampling Method	Uniform Random Sampling
Sampling size	Sensitivity
Network architecture	Sensitivity
Hidden layer transfer function	Hyperbolic Tangent
Normalization Method	[-1,1]
Error measure	RMSE
Training algorithm	Levenberg-Marquardt
Data division (train, validation, test sets)	Random, 70/15/15%
Retraining	25

RESULTS AND DISCUSSION

As already commented in the previous section, five different systems have been investigated: *Transcritical Precompression Cycle with CO_2-C_6F_6 (*from now on*, PrC CO_2-C_6F_6)*, *Recuperated Rankine Cycle with CO_2-$TiCl_4$ (RR CO_2-$TiCl_4$)*, *Transcritical Recompression Cycle with CO_2-SO_2 (RC CO_2-SO_2)*, *Recompression Cycle with sCO_2 (RC sCO_2)* and *Partial Cooling Cycle with sCO_2 (PC sCO_2)*. A sample of 5000 input combinations have been randomly generated within the limits indicated in Table 4. Afterwards, the 5000-elements sample have been simulated in Matlab to produce the corresponding thermal efficiency, which will be the target of the Neural Networks.

A sensitivity to the architecture of the ANN has been then performed. *Shallow Neural Networks* with 5, 10, 20, 30, 40 and 50 neurons in the hidden layer have been studied. *Deep Neural*

Networks with two hidden layers were also explored but dismissed in all five cases because they do not cause any significant improvement in the RMSE and/or produce overfitting of the data. For each pair of system and architecture, the number of free parameters is different as it depends on the number of inputs (see Equation 1). The selection of the best architecture has been made balancing both RMSE and cycle complexity, for a network with too many free parameters could not generalize well. Results are shown in Table 6, where the selected network architecture have been remarked in bold. The optimum number of neurons for the PrC CO_2-C_6F_6, RR CO_2-$TiCl_4$ and RC CO_2-SO_2 are 5, 5 and 20 respectively. This fact provides a preliminary information regarding the complexity of each SCARABEUS systems, being the *Transcritical Recompression* the most challenging layout for a ANN to reproduce. Indeed, the RC and PC with sCO_2 cases seems to be harder to replicate using ANN, given that a total of 30 hidden neurons are required to obtain a similar RMSE. It is worth remarking that this comparison, based only on the RMSE of the test set of the various systems, must be considered as a purely qualitative – but useful – observation, and that cannot be employed as unique indicator of the complexity of the different systems because it is influenced by a large extend by the data division performed to each training set.

Table 6. Sensitivity analysis to ANN architecture for a 5000-simulations sample. Values in the table indicate the RMSE [%] of the test set

Architecture	PrC CO_2-C_6F_6	RR CO_2-$TiCl_4$	RC CO_2-SO_2	RC sCO_2	PC sCO_2
[5]	**0.122**	**0.171**	0.266	0.652	0.530
[10]	0.116	0.171	0.171	0.371	0.302
[20]	0.115	0.171	**0.120**	0.172	0.164
[30]	0.114	0.172	0.150	**0.123**	**0.119**
[40]	0.115	0.157	0.133	0.093	0.101
[50]	0.116	0.112	0.143	0.080	0.091

A sensitivity analysis varying the size of the sample is also undertaken, with the aim of understanding whether or not 5000 simulations were sufficient to properly train the Network. The RMSE reported in Table 7 has been calculated over the 5000-sample test set in order to provide comparable results. For the PrC CO_2-C_6F_6 and RR CO_2-$TiCl_4$ systems, the small difference between the 1000 and 5000 cases, although influenced by the random division of the data, suggests that a reduced sample size might have been taken into account. Conversely, the RMSE decreases importantly with the sample size for the three remaining systems, being the optimum sample size somewhere around 4000 and 5000. For this reason, a total set of 5000 simulations have been employed in the rest of the work.

Table 7. Sensitivity analysis to the sample size. RMSE [%] measured over the 5000-test set.

System	Architecture	1000	2500	4000	5000
PrC CO_2-C_6F_6	[5]	0.177	0.125	0.127	0.122
RR CO_2-$TiCl_4$	[5]	0.188	0.174	0.175	0.171
RC CO_2-SO_2	[20]	0.678	0.288	0.138	0.12
RC sCO_2	[30]	0.247	0.192	0.125	0.123
PC sCO_2	[30]	0.261	0.168	0.135	0.119

Afterwards, the ANN developed in the previous section have been coupled with a global optimizer from the *Matlab's Global Optimization* Toolbox [40] in order to maximize thermal efficiency for various sets of boundary conditions with little computational effort. In this way,

dependence of the free parameters of each cycle with Turbine Inlet Temperature, Minimum Cycle Temperature and Maximum Cycle Pressure can be easily studied. Such free parameters, which can be optimized to maximize cycle thermal efficiency, are dopant molar fraction (for the three dopant), Precompressor pressure ratio (CO_2-C_6F_6) and split-flow factor (CO_2-SO_2). Figure 5 to Figure 7, shows the *contour maps* of the optimized parameters (from now one called *Selection maps*) obtained for the PrC CO_2-C_6F_6, RR CO_2-$TiCl_4$ and RC CO_2-SO_2 systems respectively, at a fixed maximum cycle pressure of 250 bar (SCARABEUS reference case).

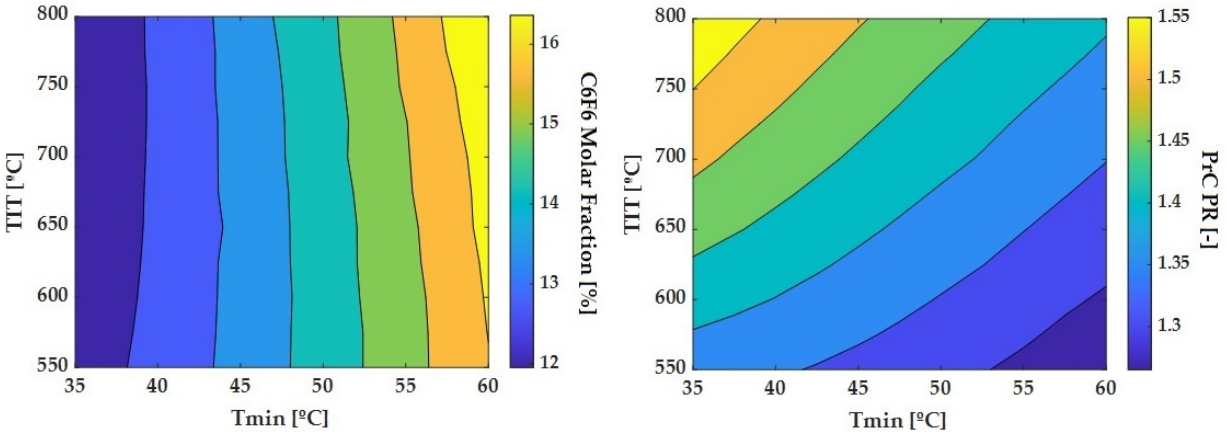

Figure 5. Selection maps for Transcritical Precompression Cycle with CO_2-C_6F_6 at 250 bar (Pmax). Left figure refers to C_6F_6 molar fraction; Right figure to Precompressor Pressure Ratio

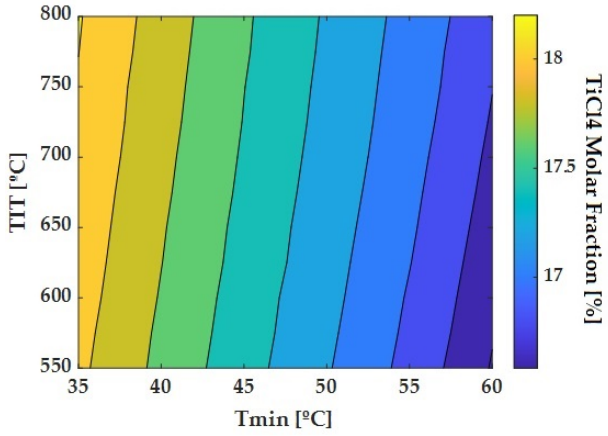

Figure 6. Selection map for Recuperated Rankine Cycle on CO_2-$TiCl_4$ at 250 bar (Pmax). Figure refers to $TiCl_4$ molar fraction

A common observation for the three systems is that optimum molar fraction strongly depends on minimum cycle temperature, but not on Turbine Inlet Temperature. For CO_2-C_6F_6, the optimum molar fraction ranges from 12 to 16.5% (Figure 5 left), increasing with Tmin. For CO_2-$TiCl_4$, the optimum molar fraction slightly varies from 18.5% to 16.5% (Figure 6), decreasing with Tmin. For CO_2-SO_2, the optimum molar fraction increases with Tmin, from 20% to 36% (Figure 7 left) and is completely conditioned by the restriction that critical temperature of the mixture has to be at least 30ºC higher than Tmin (see Candidate Dopants section).

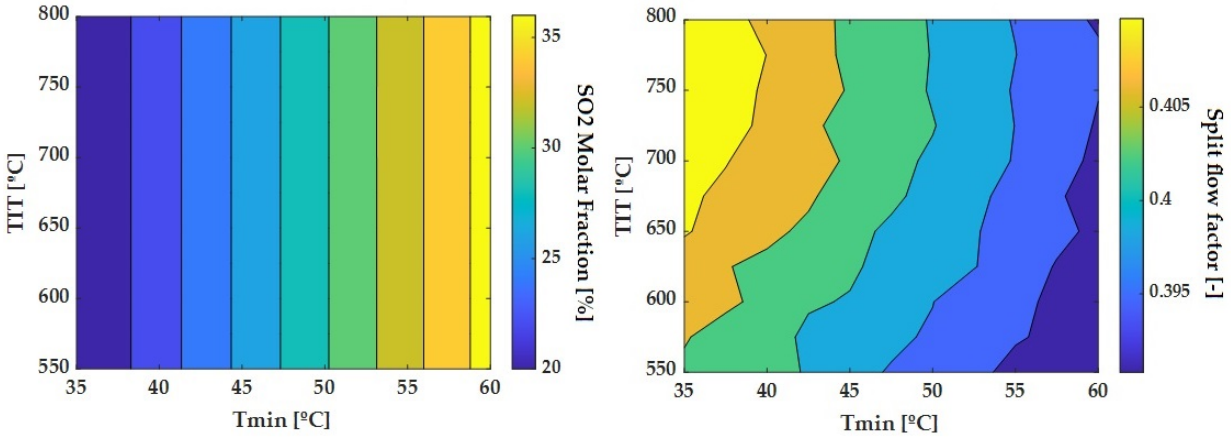

Figure 7. Selection maps for Transcritical Recompression Cycle on CO_2-SO_2 at 250 bar (Pmax). Left figure refers to SO_2 molar fraction; Right figure to Split flow factor.

The Precompressor Pressure Ratio that maximizes thermal efficiency in the PrC CO_2-C_6F_6 system increases with TIT and is inversely proportional to T_{min}, with values from 1.25 to 1.55 (Figure 5 right). The split flow factor for the RC CO_2-SO_2 (see Figure 7 right) presents more indented borders, but this is mainly due to the small variation of this parameter in the whole range of boundary conditions considered (<0.02), meaning that its optimum value is barely affected by cycle operating conditions.

To properly quantify the accuracy of the ANN predictions in these maps, two validations were performed. The first one (RMSE 1 in Table 8) refers to the RMSE of the predicted thermal efficiency with respect to the value obtained by the detailed model when simulated at the optimum design conditions predicted by the ANN (i.e., the values from the previous figures). Afterwards, the detailed models have been directly optimized for three levels of Turbine Inlet Temperature -550ºC, 625ºC and 700ºC- and multiple Minimum Cycle Temperatures –from 35ºC to 60ºC with a 2.5ºC step. The RMSE of the optimum thermal efficiency obtained by the detailed models and the thermal efficiency obtained by the ANNs were calculated (RMSE 2 in Table 8).

Table 8. Validation with the detailed model of the optimum design points. RMSE in [%]

System	Architecture	RMSE test	RMSE 1	RMSE 2
PrC CO_2-C_6F_6	[5]	0.122	0.05	0.04
RR CO_2-$TiCl_4$	[5]	0.171	0.14	0.12
RC CO_2-SO_2	[20]	0.12	0.18	0.2
RC sCO_2	[30]	0.123	0.22	0.24
PC sCO_2	[30]	0.119	0.23	0.3

A twofold conclusion can be drawn observing the trends of RMSE1 and RMSE2: firstly, both RMSE1 and RMSE2 result to be of the same order of magnitude, indicating that the optimum cases predicted by the ANN are in good accordance with the one obtained with the detailed

model (“real” optimum values); secondly, the error is extremely low for the three SCARABEUS systems – always below 0.2 percentage points (pp), and equal or below 0.05 pp for PrC CO_2-C_6F_6 – and slightly higher for the sCO_2 systems (0.2-0.3 p.p.). This circumstance confirms another observation previously made in this section, i.e. that the SCARABEUS transcritical systems seems to be easier to reproduce with the ANN than pure CO_2 supercritical ones. Once again, it is worth noting that the RMSE of the test set alone is not representative of the real prediction capability of the network, and that a more complete and thorough analysis, considering different figures of merit (not only thermal efficiency) and/or alternative data division in set, should be addressed in the future to confirm these results.

In spite of this fact, the extremely low RMSE obtained confirm the fact that the maps provided in Figure 5 to Figure 7 can be used to obtain the specifications required for the design of the different components of the cycle with an acceptable precision. In fact, the deviation in the prediction of the thermal efficiency can be considered as acceptable for real-case design scenarios, where a subsequent selection of standardized equipment would affect the optimum design point adding a higher uncertainty than that of the network.

What is more, the interest in the ANN is further demonstrated if the computational time spent in the two cases is compared. Table 9 shows a comparison between the detailed and surrogate (ANN) models of the time spent during the optimization of SCARABEUS reference case (TIT 700ºC, Tmin 50ºC and Pmax 250 bar) for the five systems studied. The fast-speed evaluation of ANN enables to perform an optimization in less than five seconds, independently of the system considered. On the contrary, the computational time required for the optimization by means of the detailed model strongly depends on the system considered due to a twofold reason: on one hand, due the numerical complexity of the model (the *Precompression Cycle* is the harder); on the other hand, due to the method employed for the calculation of fluid properties (look-up tables employed for the CO_2 mixtures are more time consuming that pure CO_2 properties obtained by Refprop). Moreover, the quantitative values shown in the second column of Table 9 depends on the tolerance required for the energy balances or, in the case of the SCARABEUS working fluid, the size of the look-up table. In any case, the reduction in computational time brought by the use of the ANN is extremely clear, and ranges from 78% for *Recuperated Rankine* - the simplest layout - up to outstanding value of 99.8%, for the *Transcritical Precompression* with CO_2-C_6F_6.

Table 9. Time requirements [s] for the optimization of the reference SCARABEUS case (TIT 700ºC, Tmin 50ºC, Pmax 250 bar) for the detailed and surrogate (ANN) models.

	Detailed model	**ANN**	**Time savings [%]**
PrC CO_2-C_6F_6	1810.5	4.3	99.8
RR CO_2-$TiCl_4$	18.4	4.1	77.7
RC CO_2-SO_2	464.9	4.4	99.1
RC sCO_2	148.9	4.4	97.0
PC sCO_2	141.5	4.8	96.6

Moreover, further studies are performed over the trained ANN, proving the flexibility and reliability of this tool. Given that the ANN for the PrC CO_2-C_6F_6 system was trained for Precompressor Pressure Ratio (PR_{PrC}) from 1 to 1.6, the ANN of this system is a superstructure including the Recuperated Rankine cycle (when $PR_{PrC} = 1$). In other words, the ANN originally

trained for a *Transcritical Precompression* cycle can be satisfactorily[2] employed to estimate, for a given dopant, the performance of a *Recuperated Rankine*. Similarly, considering the ANN trained for the *Transcritical Recompression* with CO_2-SO_2 mixture, this can be employed to reproduce a *Recuperated Rankine* if the split-flow factor is fixed to 0. Bearing this in mind, the thermal efficiency contour maps for this *Recuperated-Rankine-simulator* ANN have been obtained for the same boundary conditions of Figure 5 and Figure 7, and the thermal efficiency gains enabled by the advanced layouts with respect to the *Recuperated Rankine* are estimated.

Figure 8 (left) illustrates the thermal efficiency gain brought by the use of a *Transcritical Precompression* instead of a *Recuperated Rankine* with CO_2-C_6F_6 mixtures: it is perfectly observable that it is always higher than 1.4 pp, and it reaches a maximum for high TIT and T_{min}, confirming the superiority of the advanced layout and the results obtained in previous works by the authors [10]. On the other hand, the improvement for the CO_2-SO_2 system is even more evident (see Figure 8 (right)), with thermal efficiency gains ranging 6 to 9 pp.

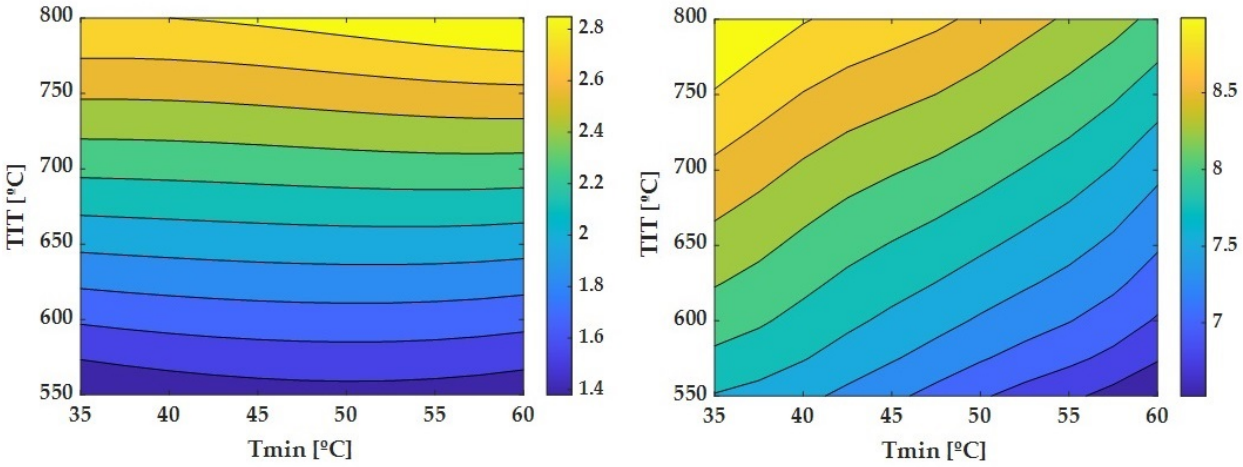

Figure 8. Thermal efficiency gains for the PrC CO_2-C_6F_6 (left) and RC CO_2-SO_2 (right) with respect to the Recuperated Rankine Cycle. Colorbars represent the gain in thermal efficiency expressed in percentage points.

Finally, a study on the optimum cycle maximum pressure is provided, repeating the optimization process considering this parameter as a free variable, and not fixing it at 250 bar (reference case for SCARABEUS project). Results in Figure 9 indicates that the thermal efficiency improvement is quite limited for the PrC CO_2-C_6F_6 and RR CO_2-$TiCl_4$, and below 1 pp for the RC CO_2-SO_2 case, confirming 250 bar as a reasonable pressure level for the SCARABEUS technology.

[2] A slight error is hereby introduced by the fact that *Precompression* cycle presents two recuperators instead of one (RR case): the ANN would consider a double pressure loss for this component. The results would therefore provide a conservative estimation of the thermal efficiency of the *Recuperated Rankine* cycle. The deviation is lesser than a relative 1%, a value of the same order of magnitude of the uncertainty brought by calculation tools. The same rationale can be applied for the *Recompression*.

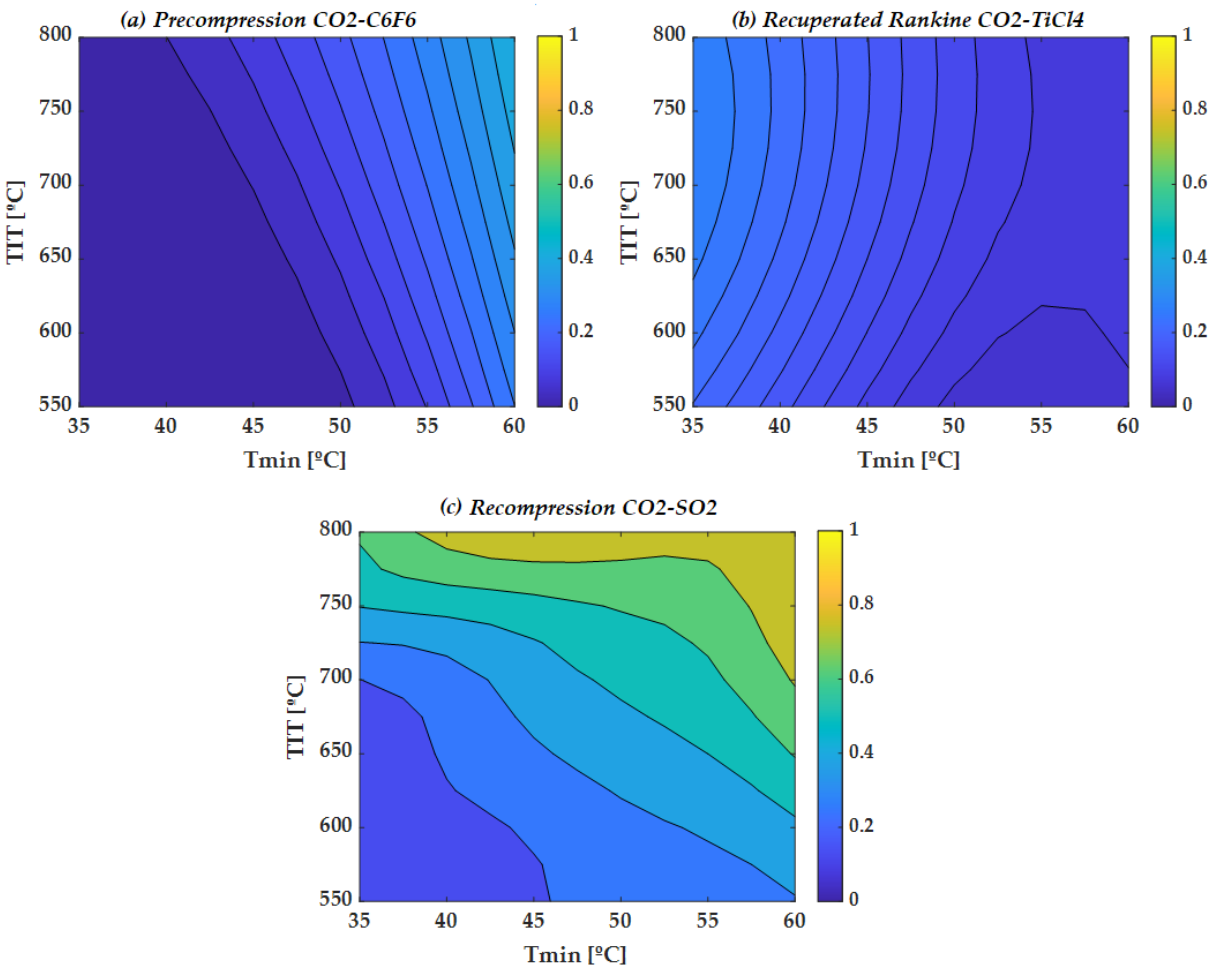

Figure 9. Thermal efficiency gains achieved optimizing maximum cycle pressure for different cycles and working fluids, with respect to their corresponding 250 bar reference case. Colorbars are expressed in percentage points.

CONCLUSIONS

The present manuscript, developed in the framework of SCARABEUS project, investigated the thermodynamic assessment and optimization by means of an Artificial Neural Network of different CO_2-based power cycles. Three dopants were studied, namely C_6F_6, $TiCl_4$ and SO_2, combined with candidate cycle layouts identified in previous works by the authors: *Transcritical Precompression* for CO_2-C_6F_6, *Recuperated Rankine* for CO_2-$TiCl_4$ and the *Transcritical Recompression* for CO_2-SO_2.

In the first part of the manuscript, the candidate dopants and cycle layouts were thoroughly presented and discussed, along with the main assumptions made and a brief description of the computational environment employed: Aspen v11 for the estimation of thermophysical properties of the mixtures, Thermoflex and Matlab for the cycle simulations and modeling (detailed models).

The second part of the manuscript dealt with the development of a comprehensive methodology to design and train Artificial Neural Networks capable of behaving as surrogate models of the detailed ones. The methodology is then applied to the three aforementioned SCARABEUS cycles and the two most promising pure sCO_2 ones, the *Recompression* and the *Partial Cooling*. Results shows that Feedforward Neural Network with one hidden layer are a very promising and

reliable tool, capable of predicting the optimum thermal efficiency with a *Root Mean Square Error* below 0.2 percentage points. An optimization routine conducted using the ANN models takes around 4-5 seconds, a value 99% lower than the one needed for a direct optimization over the detailed model.

Furthermore, it was demonstrated that the trained Neural Networks can be used with extreme flexibility. In this work, they have been employed for (1) generation of selection maps for different TIT and T_{min} levels, (2) calculation of thermal efficiency gains enabled by advanced layouts with respect to the *Recuperated Rankine Cycle* and (3) quantification of the thermal efficiency that could be achieved if maximum cycle pressure were optimized instead of fixed at 250 bar.

The key aspects having the largest impact on the design of ANN were found to be the sampling of the detailed model and the measure of the error during training. Bearing this in mind, future works will compare different sampling methods in order to guarantee that the different datasets employed during training are statistically representative of the design space and, at the same time, have the lowest size (computational burden). Additionally, future works will couple ANN with Genetic Algorithms (GA) in order to perform multi-objective optimization problems. To that end, additional ANNs will have to be trained for each system, accounting for different Key Performance Indicators such as specific work or specific CAPEX.

ACKNOWLEDGEMENTS

The SCARABEUS project has received funding from the European Union's Horizon 2020 research and innovation programme under grant agreement Nº814985. The University of Seville is also gratefully acknowledged for supporting this research through its Internal Research Programme (Plan Propio de Investigación), under contract Nº 2019/00000359. Last but not least, Junta de Andalucía is gratefully acknowledged for sponsoring the contract of Pablo Rodríguez de Arriba under the Programme for Youth Employment 2014-2020 (Phase 4).

Nomenclature

ANN	Artificial Neural Network	
BIP	Binary Interaction Parameter	
CSP	Concentrated Solar Power	
LCoE	Levelised Cost of Electricity	[€/MWh]
TIT	Turbine Inlet Temperature	[ºC]
Tmin	Minimum Cycle Temperature	[ºC]
PC	Partial Cooling Cycle	
PrC	Precompression Cycle	
Pmax	Maximum Cycle Pressure	[bar]
RC	Recompression Cycle	
RMSE	Root Mean Square Error	[p.p.]
RR	Recuperated Rankine Cycle	
ΔTmin	Minimum Temperature Difference	[ºC]
ΔP	Relative Pressure losses	[%]

$\eta_{is,T}$	Turbine isentropic efficiency	[%]
$\eta_{is,C}$	Compressor isentropic efficiency	[%]
$\eta_{is,P}$	Pump isentropic efficiency	[%]
η_{th}	Thermal efficiency	[%]

REFERENCES

[1] "SCARABEUS Project: Supercritical CARbon dioxide/Alternative fluid Blends for Efficiency Upgrade of Solar power plants. GrantID: 814985." https://cordis.europa.eu/project/id/814985 (accessed Oct. 26, 2021).

[2] "COMPASsCO2 Project: COMponents' and Materials' Performance for Advanced Solar supercritical CO2 power plants. Grant ID:958418." https://cordis.europa.eu/project/id/958418 (accessed Oct. 26, 2021).

[3] "sCO2-Flex Project: Supercritical CO2 cycle for flexible and sustainable support to the electricity system. Grant ID:764690." https://cordis.europa.eu/project/id/764690 (accessed Oct. 26, 2021).

[4] "sCO2-Hero Project: The supercritical CO2 Heat Removal System. Grandt ID: 662116." https://cordis.europa.eu/project/id/662116 (accessed Oct. 26, 2021).

[5] "sCO2-4-NPP Project: Innovative sCO2-based heat removal technology for an increased level of safety of nuclear power plants.Grant ID: 847606." https://cordis.europa.eu/project/id/847606 (accessed Oct. 26, 2021).

[6] "I-ThERM Project: Industrial Thermal Energy Recovery Conversion and Management. Grandt ID: 680599." https://cordis.europa.eu/project/id/680599 (accessed Oct. 26, 2021).

[7] "CO2OLHEAT Project: Supercritical CO2 power cycles demonstration in Operational environment Locally valorising industrialWaste Heat. Grandt ID: 10102283." https://cordis.europa.eu/project/id/101022831 (accessed Oct. 26, 2021).

[8] M. T. White, G. Bianchi, L. Chai, S. A. Tassou, and A. I. Sayma, "Review of supercritical CO 2 technologies and systems for power generation," *Applied Thermal Engineering*, vol. 185, p. 116447, Feb. 2021, doi: 10.1016/j.applthermaleng.2020.116447.

[9] F. Crespi *et al.*, "Thermal efficiency gains enabled by using CO2 mixtures in supercritical power cycles," *Energy*, vol. 238, p. 121899, Jan. 2022, doi: 10.1016/j.energy.2021.121899.

[10] F. Crespi, G. S. Martínez, P. Rodriguez de Arriba, D. Sánchez, and F. Jiménez-Espadafor, "Influence of Working Fluid Composition on the Optimum Characteristics of Blended Supercritical Carbon Dioxide Cycles," in *Volume 10: Supercritical CO2*, Virtual, Online, Jun. 2021, p. V010T30A030. doi: 10.1115/GT2021-60293.

[11] L. Wang *et al.*, "A Review of Evaluation, Optimization and Synthesis of Energy Systems: Methodology and Application to Thermal Power Plants," *Energies*, vol. 12, no. 1, p. 73, Dec. 2018, doi: 10.3390/en12010073.

[12] J. A. Bennett, A. Moisseytsev, and J. J. Sienicki, "Modeling and cycle optimization," in *Fundamentals and Applications of Supercritical Carbon Dioxide (SCO2) Based Power Cycles*, Elsevier, 2017, pp. 105–125. doi: 10.1016/B978-0-08-100804-1.00005-0.

[13] J. J. Dyreby, "Modeling the Supercritical Carbon Dioxide Brayton Cycle with Recompression," Wisconsin-Madison, 2014.

[14] P. Richter, E. Ábrahám, and G. Morin, "Optimisation of Concentrating Solar Thermal Power Plants with Neural Networks," in *Adaptive and Natural Computing Algorithms*, vol. 6593, A. Dobnikar, U. Lotrič, and B. Šter, Eds. Berlin, Heidelberg: Springer Berlin Heidelberg, 2011, pp. 190–199. doi: 10.1007/978-3-642-20282-7_20.

[15] M. V. J. J. Suresh, K. S. Reddy, and A. K. Kolar, "ANN-GA based optimization of a high ash coal-fired supercritical power plant," *Applied Energy*, vol. 88, no. 12, pp. 4867–4873,

Dec. 2011, doi: 10.1016/j.apenergy.2011.06.029.
[16] Y. Xu, C. Mao, Y. Huang, X. Shen, X. Xu, and G. Chen, “Performance evaluation and multi-objective optimization of a low-temperature CO2 heat pump water heater based on artificial neural network and new economic analysis,” *Energy*, vol. 216, p. 119232, Feb. 2021, doi: 10.1016/j.energy.2020.119232.
[17] Q. H. Deng, D. Wang, H. Zhao, W. T. Huang, S. Shao, and Z. P. Feng, “Study on performances of supercritical CO2 recompression Brayton cycles with multi-objective optimization,” *Applied Thermal Engineering*, vol. 114, pp. 1335–1342, Mar. 2017, doi: 10.1016/j.applthermaleng.2016.11.055.
[18] H. Zhao, Q. Deng, W. Huang, D. Wang, and Z. Feng, “Thermodynamic and Economic Analysis and Multi-objective Optimization of Supercritical CO2 Brayton Cycles,” *Journal of Engineering for Gas Turbines and Power*, vol. 138, no. 8, p. 081602, Aug. 2016, doi: 10.1115/1.4032666.
[19] M. M. Rashidi, O. A. Bég, A. B. Parsa, and F. Nazari, “Analysis and optimization of a transcritical power cycle with regenerator using artificial neural networks and genetic algorithms,” *Proceedings of the Institution of Mechanical Engineers, Part A: Journal of Power and Energy*, vol. 225, no. 6, pp. 701–717, Sep. 2011, doi: 10.1177/0957650911407700.
[20] R. E. Kirk and D. F. Othmer, *Encyclopedia of chemical technology*. 2003. Accessed: Nov. 09, 2021. [Online]. Available: http://www.mrw.interscience.wiley.com/emrw/9780471238966/home
[21] *Aspen Plus v11 (2021)*. Aspentech.
[22] G. Manzolini, M. Binotti, D. Bonalumi, C. Invernizzi, and P. Iora, “CO2 mixtures as innovative working fluid in power cycles applied to solar plants. Techno-economic assessment,” *Solar Energy*, vol. 181, pp. 530–544, Mar. 2019, doi: 10.1016/j.solener.2019.01.015.
[23] G. Di Marcoberardino, E. Morosini, and G. Manzolini, “Preliminary investigation of the influence of equations of state on the performance of CO2 + C6F6 as innovative working fluid in transcritical cycles,” *Energy*, vol. 238, p. 121815, Jan. 2022, doi: 10.1016/j.energy.2021.121815.
[24] G. Angelino, “Perspectives for the Liquid Phase Compression Gas Turbine,” *Journal of Engineering for Power*, vol. 89, no. 2, pp. 229–236, Apr. 1967, doi: 10.1115/1.3616657.
[25] G. Angelino, “Carbon Dioxide Condensation Cycles For Power Production,” *Journal of Engineering for Power*, vol. 90, no. 3, pp. 287–295, Jul. 1968, doi: 10.1115/1.3609190.
[26] G. Angelino, “Real Gas Effects in Carbon Dioxide Cycles,” in *ASME 1969 Gas Turbine Conference and Products Show*, Cleveland, Ohio, USA, Mar. 1969, p. V001T01A071. doi: 10.1115/69-GT-102.
[27] *Matlab v2021a (2021)*. MathWorks.
[28] *Thermoflex v29 (2021)*. Thermoflow.
[29] “Deep Learning Toolbox. MathWorks.,” 2021. https://es.mathworks.com/products/deep-learning.html (accessed Nov. 09, 2021).
[30] S. S. Haykin, *Neural networks: a comprehensive foundation*, 2nd ed. Upper Saddle River, N.J: Prentice Hall, 1999.
[31] M. T. Hagan, H. B. Demuth, M. H. Beale, and O. De Jésus, *Neural network design*, 2nd edition. s.L: Martin T. Hagan, 2014.
[32] M. Stein, “Large Sample Properties of Simulations Using Latin Hypercube Sampling,” *Technometrics*, vol. 29, no. 2, pp. 143–151, May 1987, doi: 10.1080/00401706.1987.10488205.
[33] D. Palomo Guerrero, “Aportaciones al mantenimiento predictivo de plantas de potencia: aplicación a motores diesel lentos de 2 tiempos,” Sevilla, 2017. [Online]. Available: https://idus.us.es/handle/11441/70480

[34] L. Tong, P. Bénard, Y. Zong, R. Chahine, K. Liu, and J. Xiao, “Artificial neural network based optimization of a six-step two-bed pressure swing adsorption system for hydrogen purification,” *Energy and AI*, vol. 5, p. 100075, Sep. 2021, doi: 10.1016/j.egyai.2021.100075.
[35] Y. Li, M. Jia, X. Han, and X.-S. Bai, “Towards a comprehensive optimization of engine efficiency and emissions by coupling artificial neural network (ANN) with genetic algorithm (GA),” *Energy*, vol. 225, p. 120331, Jun. 2021, doi: 10.1016/j.energy.2021.120331.
[36] A. Gharehghani, H. R. Abbasi, and P. Alizadeh, “Application of machine learning tools for constrained multi-objective optimization of an HCCI engine,” *Energy*, vol. 233, p. 121106, Oct. 2021, doi: 10.1016/j.energy.2021.121106.
[37] A. Naserbegi and M. Aghaie, “Multi-objective optimization of hybrid nuclear power plant coupled with multiple effect distillation using gravitational search algorithm based on artificial neural network,” *Thermal Science and Engineering Progress*, vol. 19, p. 100645, Oct. 2020, doi: 10.1016/j.tsep.2020.100645.
[38] B. Chegari, M. Tabaa, E. Simeu, F. Moutaouakkil, and H. Medromi, “Multi-objective optimization of building energy performance and indoor thermal comfort by combining artificial neural networks and metaheuristic algorithms,” *Energy and Buildings*, vol. 239, p. 110839, May 2021, doi: 10.1016/j.enbuild.2021.110839.
[39] G. C. Cawley and N. L. C. Talbot, “On Over-fitting in Model Selection and Subsequent Selection Bias in Performance Evaluation,” p. 29.
[40] “Global Optimization Toolbox. Mathworks,” 2021. https://es.mathworks.com/products/global-optimization.html (accessed Nov. 10, 2021).